Mechanistic Investigation of Catalytic Carbon−Carbon Bond Activation and Formation by Platinum and Palladium Phosphine Complexes

Brian L. Edelbach, Rene J. Lachicotte, and William D. Jones*

Contribution from the Department of Chemistry, University of Rochester, Rochester, New York 14627

Received September 25, 1997

Abstract: The complexes $Pt(PEt_3)_3$ and $Pd(PEt_3)_3$ cleave the C−C bond of biphenylene to give $(PEt_3)_2$Pt-(2,2′-biphenyl), **1**, and $(PEt_3)_2$Pd(2,2′-biphenyl), respectively. Heating $(PEt_3)_2$Pt(2,2′-biphenyl) in the presence of biphenylene leads to C−C cleavage of a second biphenylene to give $(PEt_3)_2$Pt(2,2′-tetraphenyl), **2,** via a Pt(IV) intermediate. **2** reductively eliminates tetraphenylene at 115 °C. At 120 °C the reaction is catalytic; $Pt(PEt_3)_3$ or **1** converts biphenylene to tetraphenylene. The intermediates in the catalytic cycle have been identified, and **1** and **2** have been characterized by X-ray analysis. Under catalytic conditions **1** and **2** approach steady-state concentrations. Kinetic analysis reveals that the steady-state concentration ratio, resting state species, and overall rate of catalysis, k_{obs}, depend on the ratio of biphenylene to PEt_3. This observation is consistent with loss of PEt_3 from **1**, resulting in the 14-electron species (PEt_3)Pt(2,2′-biphenyl), **I**. At 130 °C, **I** coordinates to PEt_3 approximately 130 times faster than it activates the C−C bond of biphenylene. The complex (depe)Pt(2,2′-biphenyl), **7** (depe = bis(diethylphosphino)ethane), does not cleave the C−C bond of biphenylene. Compound **2** is also capable of activating the C−H bonds of benzene and biphenylene to give *trans*-$(PEt_3)_2$Pt(α-biphenyl)(phenyl), **5**, and *trans*-$(PEt_3)_2$Pt(α-biphenyl)(α-biphenylenyl), **6**, respectively. Compounds **5** and **6** have been characterized by X-ray analysis. Substitution of Pd for Pt results in more rapid catalysis; $(PEt_3)_2$Pd(2,2′-biphenyl) is a very efficient catalyst (20 turnovers/h at 120 °C).

Introduction

The cleavage of C−C bonds is vitally important to the petroleum industry since it is the central step occurring in the breakdown of hydrocarbons into small organic molecules (i.e., cracking). The breaking of C−C bonds is also crucial in coal liquefaction processes such as the Exxon Donor Solvent process or the Microcat Coal Liquefaction process. Presently cracking is achieved with heterogeneous catalysts at high temperatures. Consequently, there has been renewed interest in the development of homogeneous catalysts capable of the same chemistry under mild conditions, and homogeneous systems offer an excellent opportunity to study fundamental C−C cleavage reactions.

For coal liquefaction, homogeneous systems have attracted attention due to their ability to penetrate the substrate. However, several factors impede their development. First, the metal−carbon bond resulting from C−C insertion has been calculated to be relatively weak.[1] This is certainly true for first-row transition metals, but probably not so important for third row metals such as iridium. Second, on the basis of simple steric and statistical factors, the C−H bonds surrounding the target C−C bond are kinetically more accessible. As an example, cyclopropanes have been observed to undergo C−H activation prior to rearrangement to the more stable metallacyclobutanes.[2] Third, the energy necessary to overcome the large activation barrier required for C−C bond activation often results in thermal decomposition of the metal complex prior to C−C cleavage.

To date, most examples of C−C bond cleavage by transition metals have been stoichiometric, often relying on ring strain,[3] prearomaticity,[4] or intramolecular addition in which the C−C bond is "forced" into close proximity to the metal.[5] Of this latter variety, Milstein and co-workers have discovered a system that is capable of removing a methyl group from an aromatic ring attached to a phosphine ligand. β-Alkyl migration has been observed with electrophilic early transition metal complexes.[6] *Catalytic* C−C bond cleavage is much less common.[5,7] Vollhardt et al. achieved a catalytic reaction in which tetraphenylene

(1) (a) Crabtree, R. H. In *The Chemistry of Alkanes and Cycloalkanes*; Patai, S., Rappoport, Z., Eds.; John Wiley & Sons: New York, 1992; p 653. (b) Crabtree, R. H. *Chem Rev.* **1985**, *85*, 245. (c) Halpern, J. *Acc. Chem. Res.* **1982**, *15*, 238−244. (d) Pilchner, G.; Skinner, H. A. In *The Chemistry of the Metal−Carbon Bond*; Patai, S., Ed.; John Wiley & Sons: New York, 1982.

(2) Periana, R. A.; Bergman, R. G. *J. Am. Chem. Soc.* **1986**, *108*, 7346−7355 and references therein.

(3) (a) Adams, D. M.; Chatt, J.; Guy, R. G.; Sheppard, N. *J. Chem. Soc.* **1961**, 738−742. (b) Bailey, N. A.; Gillard, R. D.; Keeton, M.; Mason, R.; Russell, D. R. *J. Chem. Soc., Chem. Commun.* **1966**, 396−398. (c) McQuillin, F. J.; Powell, K. C. *J. Chem. Soc., Dalton Trans.* **1972**, 2123−2129. (d) Barretta, A.; Cloke, F. G. N.; Feigenbaum, A.; Green, M. L. H.; Gourdon, A.; Prout, K. *J. Chem. Soc., Chem. Commun.* **1981**, 156−158. (e) Baretta, A.; Chong, K. S.; Cloke, F. G. N.; Feigenbaum, A.; Green, M. L. H. *J. Chem. Soc., Dalton Trans.* **1983**, 861−864. (f) Flood, T. C.; Statler, J. A. *Organometallics* **1984**, *3*, 1795−1803. (g) Eisch, J. J.; Piotrowski, A. M.; Han, K. I.; Krüger, C.; Tsay, Y. H. *Organometallics* **1985**, 224−231. (h) Schwager, H.; Spyroudis, S.; Vollhardt, K. P. C. *J. Organomet. Chem.* **1990**, *382*, 191−200. (i) Lu, Z.; Jun, C.−H.; de Gala, S. R.; Sigalas, M.; Eisenstein, O.; Crabtree, R. H. *J. Chem. Soc., Chem. Commun.* **1993**, 1877−1880. (j) Lu, Z.; Jun, C.-H.; de Gala, S. R.; Eisenstein, O.; Crabtree, R. H. *Organometallics* **1995**, *14*, 1168−1175. (k) Perthuisot, C.; Edelbach, B. E.; Zubris, D. L.; Jones, W. D. *Organometallics* **1997**, *16*, 2016−2023.

(4) (a) Kang, J. W.; Moseley, K.; Maitlis, P. J. *J. Am. Chem. Soc.* **1969**, *91*, 5970−5977. (b) Benfield, F. W. C.; Green, M. L. H. *J. Chem. Soc., Dalton Trans.* **1974**, 1324−1331. (c) Eilbracht, P. *Chem. Ber.* **1976**, *109*, 1429. (d) Crabtree, R. H.; Dion, R. P.; Gibboni, D. J.; McGrath, D. V.; Holt, E. M. *J. Am. Chem. Soc.* **1986**, *108*, 7222−7227. (e) Hemond, R. C.; Hughes, R. P.; Locker, H. B. *Organometallics* **1986**, *5*, 2391−2392. (f) Jones, W. D.; Maguire, J. A. *Organometallics* **1987**, *6*, 1301−1311.

S0002-7863(97)03368-4 CCC: $15.00
Published on Web 03/12/1998

and derivatives of tetraphenylene were catalytically formed from biphenylene derivatives using $Ni(COD)(PMe_3)_2$.[3] On the basis spectroscopic data and earlier work by Eisch et al.,[3g] the mechanism shown in eq 1 was proposed. However, no detailed

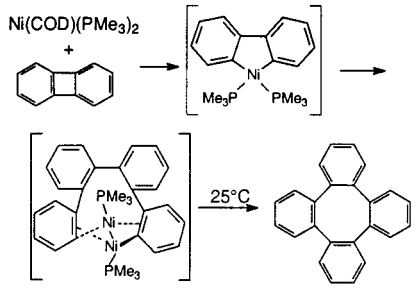

(1)

mechanistic studies were performed.

Here we report that several Pt and Pd complexes are capable of catalyzing the formation of tetraphenylene from biphenylene. In an effort to increase our understanding of the conditions necessary to cleave strong aryl−aryl bonds, a detailed mechanistic study was performed to determine the operating catalytic cycle. We anticipated that aryl−aryl bonds should be among the easiest to cleave for two reasons. First, while the aryl−aryl C−C bond is one of the strongest C−C bonds, the oxidative addition product would contain two strong M−aryl bonds, which should make the cleavage of this type of bond one of the most favorable. (A similar line of reasoning has been used to explain why the strong aryl−H bond is one of the easiest to undergo C−H activation.[8]) Second, the π-system of a biaryl substrate offers the opportunity for coordination prior to C−C insertion, thereby decreasing the kinetic barrier to C−C oxidative addition. Biphenylene offers several advantages as a substrate for studying C−C cleavage. In addition to having two aryl−aryl C−C bonds, it is also a strained ring molecule, and insertion into the C−C bond will be even more favorable than into a simple biaryl C−C bond.

Results

Thermal Reaction of $Pt(PEt_3)_3$ with Biphenylene. The thermolysis of $Pt(PEt_3)_3$ in benzene-d_6 with 10 equiv of biphenylene (**BP**) at 120 °C resulted in the catalytic formation of tetraphenylene (0.135 turnovers/day, eq 2). The ^{1}H NMR spectrum was complicated throughout the reaction. Early in the catalytic cycle, the $^{31}P\{^1H\}$ NMR spectrum revealed the presence of two Pt bound phosphine species as well as free PEt_3.

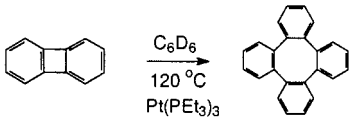

(2)

The major Pt bound phosphine species was found at δ 8.44 (s, $J_{Pt-P} = 1922$ Hz); the minor species was found at δ −0.44 (s, $J_{Pt-P} = 3173$ Hz).

Identification of Intermediates in the Catalytic Reaction. The major species at δ 8.44 was formed stoichiometrically in high yield by heating $Pt(PEt_3)_3$ in the presence of biphenylene at 80 °C. Free PEt_3 was also formed in this reaction. The ^{1}H NMR spectrum showed no hydride resonances, suggesting that the first intermediate formed in the catalytic reaction was $(PEt_3)_2$-Pt(2,2′-biphenyl), **1**, resulting from C−C bond activation of biphenylene (eq 3). Compound **1** was independently synthe-

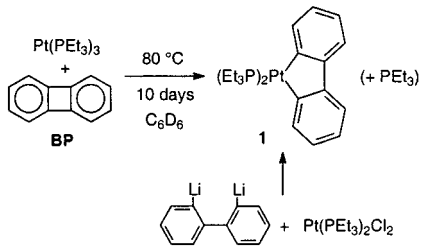

(3)

sized by reacting 2,2′-dilithiobiphenyl with *cis*-$(PEt_3)_2PtCl_2$. The ^{1}H and ^{31}P NMR spectra of **1** were identical to the major species formed in the reaction shown in eq 2. The aromatic region of the ^{1}H NMR spectrum of **1** exhibited an ABCD pattern, with the two deshielded aromatic protons ortho to the Pt−C bond found at δ 7.501 (dd, $J_{Pt-H} = 48.6$, $J_{H-H} = J_{P-H} = 7.2$ Hz, 2 H). Three other resonances corresponding to the six remaining aromatic protons were observed at δ 7.405 (d, $J_{H-H} = 7.6$ Hz), 6.999 (t, $J_{H-H} = 7.2$ Hz), and 6.880 (t, $J_{H-H} = 7.2$ Hz).

The X-ray structure of **1** was determined (Figure 1). The solid-state structure shows a distorted square planar complex with a pseudo-2-fold axis bisecting the two phosphines and the biphenyl. The distortion is best described by a twist angle of 26.5° between the planes defined by Pt, C(1), C(12) and Pt, P(1), P(2). Alternatively, the four ligating atoms lie an average of 0.33 Å above and below the best plane of the PtL_4 moiety. The bond angles about the platinum deviate from ideal square planar geometry, ranging from 79.9(2)° to 97.08(4)°.

Heating complex **1** at 80 °C in the presence of biphenylene (with no added phosphine) led to the quantitative formation of $(PEt_3)_2Pt(2,2'$-tetraphenyl) (**2**) (eq 4). The ^{1}H and ^{31}P NMR

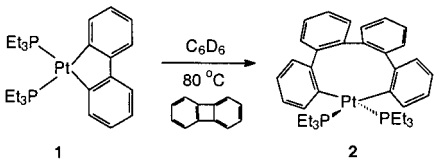

(4)

spectra of **2** matched that of the minor species formed in the reaction shown in eq 2. The aromatic region of the ^{1}H NMR spectrum of **2** showed the two downfield ortho protons at δ 7.441 (d, $J_{Pt-H} = 34.2$, $J_{H-H} = 7.2$ Hz). The rest of the aromatic region integrated to 14 protons; however, individual proton assignments were not possible due to the overlap of proton resonances. The large platinum−phosphorus coupling of **2** as compared to **1** suggested that the phosphines were trans to one another in **2**. Large platinum−phosphorus coupling of trans

(5) (a) Suggs, J. W.; Jun, C.−H. *J. Chem. Soc., Chem. Commun.* **1985**, 92−93. (b) Gozin, M.; Weisman, A.; Ben−David, Y.; Milstein, D. *Nature* **1993**, *364*, 699−701. (c) Gozin, M.; Aizenberg, M.; Liou, S.-Y.; Weisman, A.; Ben−David, Y.; Milstein, D. *Nature* **1994**, *370*, 42−44. (d) Liou, S.−Y.; Gozin, M.; Milstein, D. *J. Chem. Soc., Chem. Commun.* **1995**, 1165−1166. (e) Liou, S.−Y.; Gozin, M.; Milstein, D. *J. Am. Chem. Soc.* **1995**, *117*, 9774−9775. (f) Rybtchinski, B.; Vigalok, A.; Ben−David, Y.; Milstein, D. *J. Am. Chem. Soc.* **1996**, *118*, 12406−12415. (g) van der Boom, M. E.; Kraatz, H.-B.; Ben−David, Y.; Milstein, D. *J. Chem. Soc., Chem. Commun.* **1996**, 2167−2168. (h) Gandelman, M.; Vigalok, A.; Shimon, L. J. W.; Milstein, D. *Organometallics* **1997**, *16*, 3981−3986.

(6) Watson, P. L.; Roe, D. C. *J. Am. Chem. Soc.* **1982**, *104*, 6471−6473. Bunel, E.; Burger, B. J.; Bercaw, J. E. *J. Am. Chem. Soc.* **1988**, *110*, 976−978.

(7) (a) Noyori, R.; Kumagai, Y.; Umeda, I.; Takaya, H. *J. Am. Chem. Soc.* **1972**, *94*, 4018. (b) Kaneda, K.; Azuma, H.; Wayaku, M.; Teranishi, S. *Chem. Lett*. **1974**, 215. (c) Fujimura, T.; Aoki, S.; Nakamura, E. *J. Org. Chem.* **1991**, *56*, 2809 and references therein. (d) Huffman, M. A.; Liebeskind, L. S. *J. Am. Chem. Soc.* **1991**, *113*, 2771. (e) Perthuisot, C.; Jones, W. D. *J. Am. Chem. Soc.* **1994**, *116*, 3647−3648. (f) Murakami, M.; Amii, H.; Shigeto, K.; Ito, Y. *J. Am. Chem. Soc.* **1996**, *118*, 8285−8290.

(8) Jones, W. D.; Feher, F. J. *Acc. Chem. Res.* **1989**, *22*, 91−100.

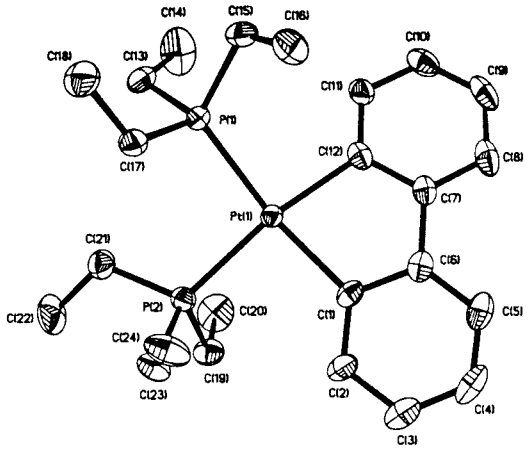

Figure 1. ORTEP drawing of **1**. Ellipsoids are shown at the 30% level. Hydrogen atoms have been omitted for clarity.

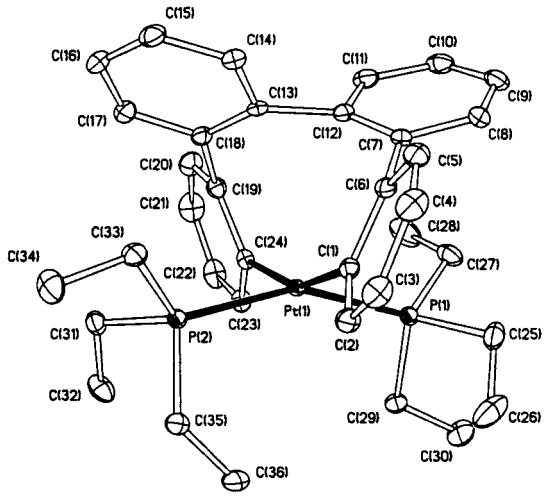

Figure 2. ORTEP drawing of **2**. Ellipsoids are shown at the 30% level. Hydrogen atoms have been omitted for clarity.

phosphines vs phosphines trans to an alkyl or aryl group has been established empirically, and is owed in part to the larger trans effect of an alkyl or aryl group relative to a phosphine group.[9]

The structure of **2** was confirmed by X-ray crystallography (Figure 2). The solid-state structure was very distorted from a square planar geometry (0.46 Å average deviation from a square plane). The P(1)−Pt(1)−P(2) bond angle was 154.27(3)° and the C(1)−Pt(1)−C(24) angle was 157.06(12)°. A twist angle of 33.7° was found between the planes defined by the atoms Pt(1), P(1), C(1) and atoms Pt(2), P(2), C(24).

Complex **1** catalyzes the formation of tetraphenylene from biphenylene. When complex **1** was heated at 120 °C in the presence of excess biphenylene, the catalytic formation of tetraphenylene was 5× more rapid than when $Pt(PEt_3)_3$ was employed as the catalyst (0.6 turnovers/day), suggesting that free phosphine inhibits the catalysis. Furthermore, when **1** was used as the catalyst, the resting state species in the catalytic cycle was complex **2** (no **1** was seen by ^{1}H or ^{31}P NMR spectroscopy).

Compound **2** was also shown to be an intermediate in the catalytic formation of tetraphenylene. When **2** was heated at 120 °C in the presence of excess biphenylene, tetraphenylene was formed catalytically with the same turnover rate given by complex **1**. The resting state species was also compound **2**.

Table 1. k_{obs} for Reductive Elimination of Tetraphenylene from **2** (0.023 M) in Toluene-d_8 at 115.5 °C

$[PEt_3]$ (M)	k_{obs} (s^{-1})	$[PEt_3]$ (M)	k_{obs} (s^{-1})	$[PEt_3]$ (M)	k_{obs} (s^{-1})
0	2.50×10^{-6}	0.044	2.25×10^{-6}	0.29	2.27×10^{-6}
0.022	2.22×10^{-6}	0.15	2.38×10^{-6}	0.49	2.39×10^{-6}

Scheme 1

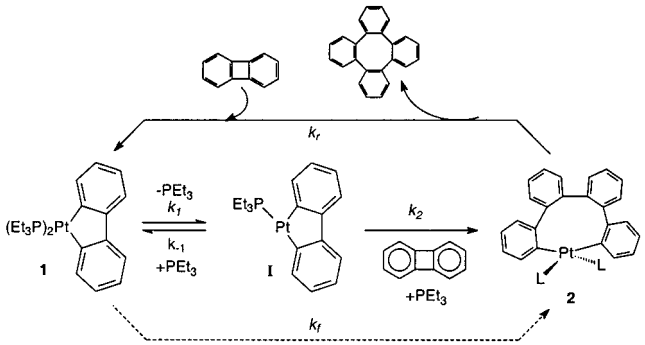

Reductive Elimination Kinetics from 2. Added phosphine has two pronounced effects on the catalytic formation of tetraphenylene. First, free phosphine inhibits the rate of formation of tetraphenylene. Second, with additional phosphine present, the resting state changes from **2** to **1**. The first step in understanding these observations was to monitor the rate of reductive elimination of tetraphenylene from complex **2**. Sealed NMR tubes containing toluene-d_8 solutions of complex **2** (0.023 M) were prepared with various phosphine concentrations (0−0.48 M) and heated at 115.5 °C. The disappearance of **2** was followed by ^{1}H NMR spectroscopy to 3 half-lives. The reactions all showed the concomitant formation of tetraphenylene. $Pt(PEt_3)_3$ was also produced in those samples with added phosphine; with no added phosphine collodial platinum was formed.[10] The rate of disappearance of **2** followed first-order kinetics and was not affected by the phosphine concentration (Table 1). The average rate constant for all reactions was calculated to be $2.34(11) \times 10^{-6}$ s^{-1}.

Kinetics. The next objective was to probe the effect of added phosphine on the rate of formation of **2** from **1** in the presence of biphenylene at 80 °C, a temperature at which reductive elimination of tetraphenylene from **2** does not occur. To our surprise even the slightest amount of added phosphine severely inhibited the rate of formation of **2**. At 80 °C and 0.000625 M PEt_3 (0.025 equiv based on **1**), no detectable reaction could be observed even after 24 h. Therefore, the concentrations of **1** and **2** were monitored under catalytic conditions at 130 °C in *p*-xylene-d_{10} with various ratios of biphenylene to PEt_3. The concentration of PEt_3 was constant throughout the reaction since it is not consumed, and pseudo-first-order concentrations of biphenylene were used to ensure constant concentrations early on in the cycle. Figure 3 shows the results of this study. In all cases the concentrations of **1** and **2** approach steady-state values as the catalytic cycle progresses.

Given the inhibition of added phosphine on the formation of **2** and the intermediates identified, the following general kinetic scheme for catalysis is proposed (Scheme 1). The first step involves reversible dissociation of phosphine to give a three-coordinate intermediate, **I**, which can either recoordinate phos-

(9) Pregosin, P. S.; Kunz, R. W. In *NMR 16 Basic Principles and Progress: ^{31}P and ^{13}C NMR of Transition Metal Phosphine Complexes*; Diehl, P., Fluck, E., Kosfeld, R., Eds.; Springer-Verlag: Berlin, 1979; pp 42−43.

(10) DiCosimo, R.; Whitesides, G. M.; *J. Am. Chem. Soc.* **1982**, *104*, 3601−3607.

Table 2. Results of Kinetic Analysis of Figure 3[a]

[BP]	[PEt_3]	[BP]/[PEt_3]	k_{obs}, s^{-1}	$[\mathbf{2}]_{ss}/[\mathbf{1}]_{ss}$	k_r, s^{-1}	k_f, s^{-1}
0.1	0.01	10	1.46×10^{-5}	0.28	1.14×10^{-5}	3.24×10^{-6}
0.2	0.02	10	1.46×10^{-5}	0.22	1.19×10^{-5}	2.66×10^{-6}
0.3	0.03	10	1.46×10^{-5}	0.24	1.17×10^{-5}	2.82×10^{-6}
0.1	0.02	5	1.04×10^{-5}	0.13	9.22×10^{-6}	1.22×10^{-6}
0.3	0.0135	22	1.83×10^{-5}	0.53	1.20×10^{-5}	6.33×10^{-6}

[a]The concentration of **1** for each run was 0.023 M.

phine or react with biphenylene to give **2**. The forward rate constant, k_f, represents a composite of these steps. The reverse rate constant, k_r, is the rate constant for reductive elimination of tetraphenylene from **2** to generate "$(PEt_3)_2Pt$" which rapidly C−C activates biphenylene to regenerate **1**. Since only **1** and **2** are observed in the catalytic reaction, a steady-state approximation can be applied to **I**, giving the rate law shown in eq 5 and the expression for k_f (eq 6). Equation 6 reveals the

$$-\frac{d[\mathbf{1}]}{dt} = k_f[\mathbf{1}] - k_r[\mathbf{2}] \quad (5)$$

$$k_f = \frac{k_1}{1 + k_{-1}[PEt_3]/k_2[\mathbf{BP}]} \quad (6)$$

source of the inverse dependence on phosphine concentration of the formation of **2** (at a constant **BP** concentration) observed experimentally at 80 °C.

Since the concentrations of **1** and **2** change rapidly at first, but then change only slowly over the course of the catalysis, the overall kinetics can be treated as an approach to steady state. Once a steady-state concentration is reached $d[\mathbf{1}]/dt \approx 0$; therefore, eq 5 can be rewritten as eq 7, where $[\mathbf{1}]_{ss}$ and $[\mathbf{2}]_{ss}$ are the concentrations of **1** and **2** at steady state. The application of mass balance and substitution into eq 5 leads to eqs 8 and 9 (see the Experimental Section). Integration of eq 8 gives eq 10 from which k_{obs} can be obtained. This treatment indicates

$$k_f[\mathbf{1}]_{ss} = k_r[\mathbf{2}]_{ss} \quad (7)$$

$$-\frac{d[\mathbf{1}]}{dt} = (k_{obs})([\mathbf{1}] - [\mathbf{1}]_{ss}) \quad \text{where} \quad k_{obs} = k_f + k_r \quad (8)$$

$$k_{obs} = \left(\frac{k_1}{1 + k_{-1}[PEt_3]/k_2[\mathbf{BP}]}\right) + k_r \quad (9)$$

$$[\mathbf{1}] = ([\mathbf{1}]_o - [\mathbf{1}]_{ss})e^{-k_{obs}t} + [\mathbf{1}]_{ss} \quad (10)$$

that k_{obs} should be affected by the *ratio* of biphenylene to PEt_3 and not by the individual concentrations of biphenylene and PEt_3 (eq 9). The data for each experiment in Figure 3 were fit to eq 10 using a least-squares approach in which k_{obs}, $[\mathbf{1}]_o$, and $[\mathbf{1}]_{ss}$ were allowed to vary. The values of k_{obs} obtained are shown in Table 2. Parts a−c of Figure 3 display reactions at a constant biphenylene to phosphine ratio (10:1), with each ratio being generated from different concentrations of biphenylene and PEt_3. Table 2 indicates that the values of k_{obs} are nearly equal for all three runs. Furthermore, the steady-state ratios, $[\mathbf{2}]_{ss}/[\mathbf{1}]_{ss}$, are approximately the same for all three runs. Decreasing the biphenylene to PEt_3 ratio to 5:1 (Figure 3d) leads to a reduction in k_{obs}, as predicted by eq 9, as well as a reduction in the steady-state ratio. Increasing the biphenylene to PEt_3 ratio to 22:1 (Figure 3e) leads to an increase in k_{obs}, and an increase in the steady-state ratio, $[\mathbf{2}]_{ss}/[\mathbf{1}]_{ss}$.

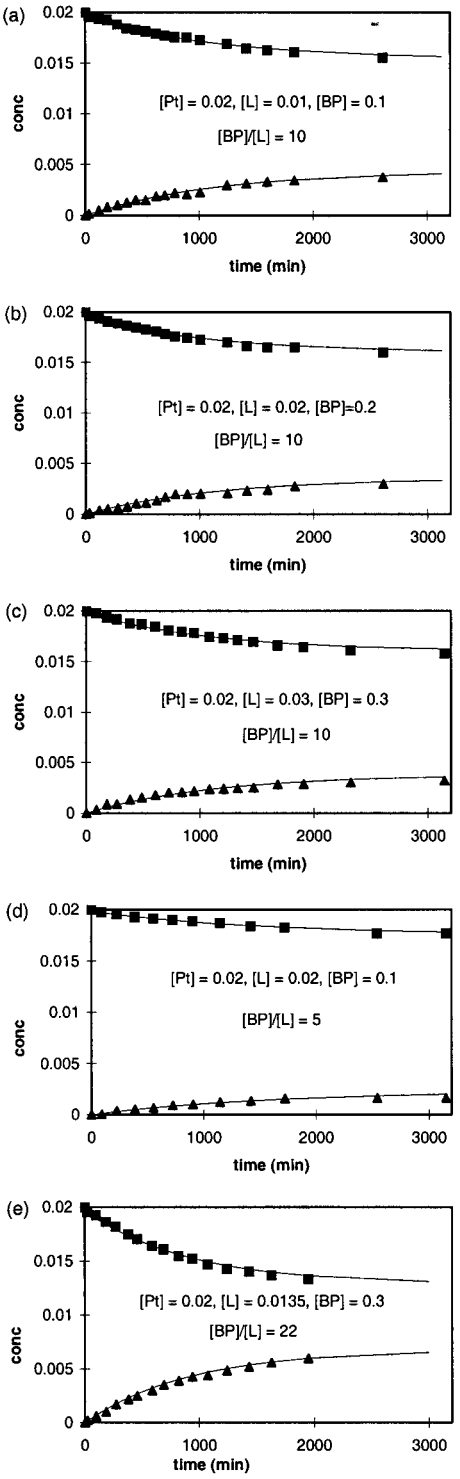

Figure 3. Concentration vs time plots of **1** (■) and **2** (▲) at varying biphenylene (**BP**) and PEt_3 (L) concentrations during the catalytic formation of tetraphenylene at 130 °C in *p*-xylene-d_{10}.

The rate constant k_r was calculated by using eq 11 (see the Experimental Section), and k_f was determined by rearranging

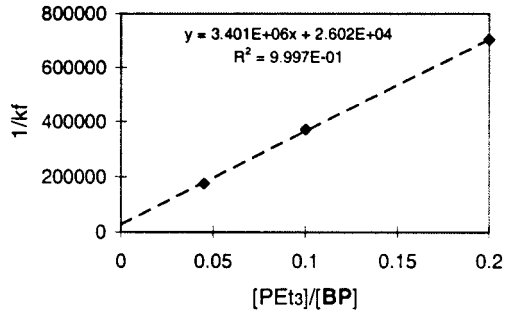

Figure 4. $1/k_f$ vs $[PEt_3]/[BP]$ for the conversion of **1** to **2** at 130 °C.

eq 7 to give eq 12. These results are also shown in Table 2.

$$k_r = k_{obs}/(1 + [\mathbf{2}]_{ss}/[\mathbf{1}]_{ss}) \quad (11)$$

$$k_f = ([\mathbf{2}]_{ss}/[\mathbf{1}]_{ss})k_r \quad (12)$$

The reverse rate constant, k_r, was also determined independently by monitoring the rate of reductive elimination of tetraphenylene from **2** at 130 °C in *p*-xylene-d_{10}. The value of k_r was 1.08(3) $\times$ 10^{-5} s^{-1}, in very close agreement to the values determined from fits of the data displayed in Figure 3. Equation 6 predicts that k_f is also dependent on the *ratio* of biphenylene to PEt_3, and that decreasing this ratio leads to a decrease in k_f and vice versa. Table 2 shows that this was indeed the case.

Taking the reciprocal of eq 6 leads to eq 13. A plot of $1/k_f$ vs $[PEt_3]/[\mathbf{BP}]$ at 130 °C is shown in Figure 4. The values k_f

$$\frac{1}{k_f} = \frac{k_{-1}}{k_1 k_2}\frac{[PEt_3]}{[\mathbf{BP}]} + \frac{1}{k_1} \quad (13)$$

were determined by using eq 12 (with the steady-state ratios from Table 1, and k_r = 1.08(3) $\times$ 10^{-5} s^{-1}). The intercept allowed for the determination of k_1 (3.84 $\times$ 10^{-5} s^{-1}), although the error is fairly large relative to the magnitude of k_1. The slope and k_1 provide an approximate value for the branching ratio (k_{-1}/k_2) of 131. That is, the coordinatively unsaturated intermediate **I** recoordinates to phosphine 131 times faster than it reacts with biphenylene, thereby explaining the observed phosphine inhibition.

Evidence for a Pt(IV) Intermediate. Although complexes **1** and **2** have been identified as intermediates during the catalysis, the question of how **1** goes on to **2** remains open. One possibility is that **1** forms **2** via the Pt(IV) species **3**. Rapid

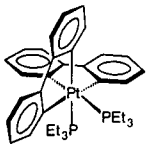

3

reductive elimination of adjacent aryl groups from **3** would generate **2**. To test this hypothesis, the Pt(IV) species *trans*-$(PEt_3)_2$Pt(2,2′-biphenyl)Br_2 (**4**) was formed by adding Br_2 to complex **1** (eq 14). Complex **4** was characterized by ^1H and

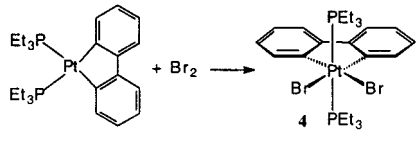

(14)

^{31}P NMR spectroscopy, X-ray crystallography, and elemental

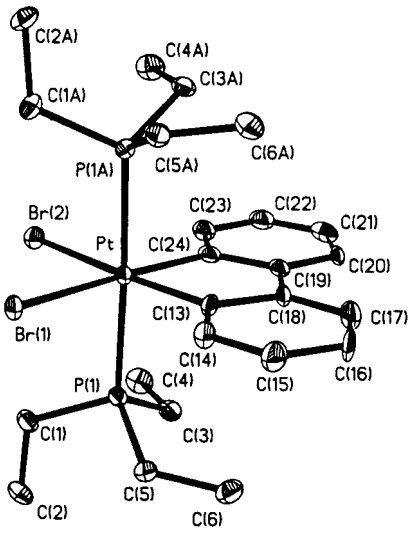

Figure 5. ORTEP drawing of **4**. Ellipsoids are shown at the 30% level. Hydrogen atoms have been omitted for clarity.

anaylsis. The $^{31}P\{^1H\}$ NMR spectrum of **4** appears as a singlet at δ −11.44 with a J_{Pt-P} of 1749 Hz. The lower J_{Pt-P} coupling of Pt(IV) vs Pt(II) species is well established.[9] The *trans* orientation of the phosphine ligands was confirmed by X-ray crystallography (Figure 5).

A diethyl ether solution of 2,2′-dilithiobiphenyl was added to a benzene solution of **4** in an attempt to form complex **3** (eq 15). All attempts to isolate **3** failed. Therefore, the mixture of

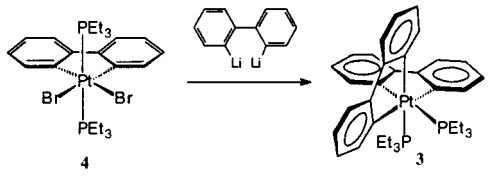

(15)

2,2′-dilithiobiphenyl and **4** was stirred for 15 min, the resulting suspension was quickly filtered, and the solvent was removed under high vacuum. The solid was dissolved in benzene, and a $^{31}P\{^1H\}$ NMR spectrum was acquired. The spectrum revealed the presence of two Pt bound phosphine species in approximately equal ratios. One species was identified as complex **2** on the basis of the $^{31}P\{^1H\}$ NMR spectrum. The other species appeared as a singlet at δ −31.64 (J_{Pt-P} = 1242 Hz). The lower Pt−P coupling constant of this species relative to **4** suggests that the phosphines are trans to aryl groups. At room temperature, this species disappeared with the concomitant formation of complex **2**, providing strong evidence that **3** is an intermediate in the catalytic cycle. The addition of several equivalents of PEt_3 (4 mM) did not inhibit this interconversion.

Side Reactions with C_6D_6 and Biphenylene. During the course of catalysis by heating **1** with excess biphenylene in C_6D_6 solvent, two new minor platinum phosphine complexes slowly appeared. The first complex formed relatively early on, and its $^{31}P\{^1H\}$ NMR spectrum displayed a singlet at δ 4.40 (s, J_{Pt-P} = 2871 Hz). The second complex grew in very slowly, and its $^{31}P\{^1H\}$ NMR spectrum showed a singlet at δ 5.02 (s, J_{Pt-P} = 2805 Hz). The first complex was formed independently by heating **1** in C_6D_6 at 130 °C. The complex was identified as *trans*-$(PEt_3)_2$Pt(α-biphenyl)(phenyl), **5**, a square planar platinum-(II) species with trans phosphines and trans biphenyl and phenyl groups. The solid-state structure was determined by X-ray crystallography (Figure 6). This structure is consistent with the larger Pt−P coupling constant of complex **5** relative to **1**, given

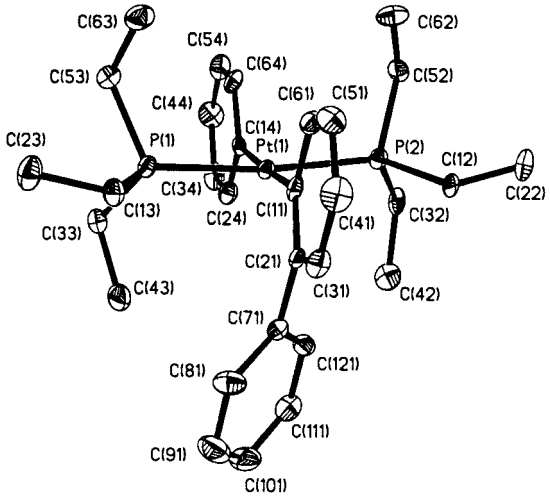

Figure 6. ORTEP drawing of **5**. Ellipsoids are shown at the 30% level. Hydrogen atoms have been omitted for clarity.

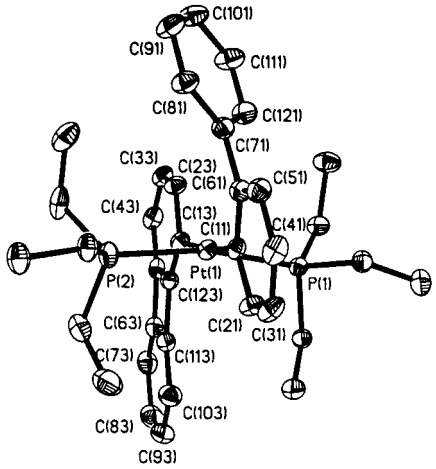

Figure 7. ORTEP drawing of **6**. Ellipsoids are shown at the 30% level. Hydrogen atoms have been omitted for clarity.

that alkylphosphines are not as efficient trans directors as aryl groups. The ^{1}H NMR spectrum of **5-*d*$_6$** isolated from the catalytic reaction in C_6D_6 integrated to eight protons in the aromatic region. This is consistent with a fully deuterated phenyl group and one deuterium on the biphenyl group. The second species, **6**, was isolated by combining several catalytic reaction mixtures which had gone to completion and separating the components by column chromotagraphy. The solid-state structure of **6** was determined by X-ray crystallography (Figure 7). Complex **6** was identified as *trans*-$(PEt_3)_2$Pt(α-biphenyl)-(α-biphenylenyl), also a square planar platinum (II) species with trans phosphines and trans biphenyl and biphenylenyl groups. Both **5** and **6** were heated at 120 °C in the presence of excess biphenylene, but no reaction occurred in either case. Furthermore, the formation of both complexes was inhibited by the presence of excess phosphine. The formation of complex **5** can be avoided by running the catalytic reaction in THF-d_8, toluene-d_8, or *p*-xylene-d_{10}.

Reaction of (depe)Pt(2,2′-biphenyl). (depe)Pt(2,2′-biphenyl), **7** (depe = bis(diethylphosphino)ethane), was synthesized from (depe)$PtCl_2$ and 2,2′-dilithiobiphenyl in a manner similar to that of complex **1**. A structure of the complex shows the expected square planar geometry with only a slight deviation from planarity (±0.15 Å, average, Figure 8). A THF-d_8 solution of **7** and excess biphenylene was heated at 130 °C for one week during which time no reaction was observed.

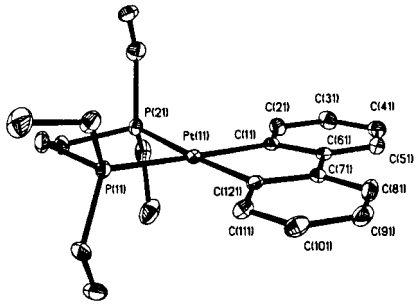

Figure 8. ORTEP drawing of **7**. Ellipsoids are shown at the 30% level. Hydrogen atoms have been omitted for clarity.

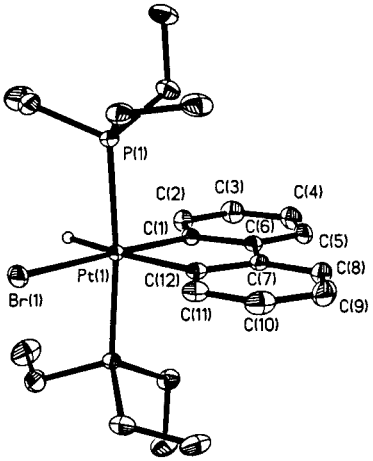

Figure 9. ORTEP drawing of **8**. Ellipsoids are shown at the 30% level. Hydrogen atoms have been omitted for clarity except the hydride ligand.

Catalysis with Pd Complexes. The effect of changing the metal was also probed by heating $Pd(PEt_3)_3$ in the presence of excess biphenylene in C_6D_6. As with $Pt(PEt_3)_3$, tetraphenylene was formed catalytically. With $Pd(PEt_3)_3$ the turnover rate was considerably faster (16 turnovers/day at 120 °C in C_6D_6). Furthermore, the $^{31}P\{^1H\}$ NMR spectrum consisted of only two singlets throughout the course of the catalysis. One singlet corresponded to free PEt_3; the other resonance was assigned as **(**$PEt_3)_2$Pd(2,2′-biphenyl) (δ 4.94). The assignment of the Pd species was based on its ^{1}H NMR spectrum. The aromatic region displayed a very similar ABCD pattern to that observed for **(**$PEt_3)_2$Pt(2,2′-biphenyl). The splitting patterns of the methyl and methylene groups on the phosphine were identical to those of the Pt analogue. **(**$PEt_3)_2$Pd(2,2′-biphenyl) was formed stoichiometrically by heating $Pd(PEt_3)_3$ at 60 °C in the presence of approximately 1 equiv of biphenylene. **(**$PEt_3)_2$Pd(2,2′-biphenyl) proved to be the most efficient catalyst for the formation of tetraphenylene from biphenylene (20 turnovers/h at 120 °C in C_6D_6). No side products were observed during the course of catalysis.

Discussion

Tetraphenylene is formed catalytically from biphenylene using $Pt(PEt_3)_3$. The catalytic cycle outlined in Scheme 2 is proposed on the basis of kinetic analysis and the identification of complexes **1**, **2**, and **3** as intermediates in the cycle. The first step of the catalytic reaction is loss of phoshine from $Pt(PEt_3)_3$ to give the putative species $Pt(PEt_3)_2$ which rapidly inserts into the C−C bond of biphenylene to give intermediate **1**. Reversible loss of phosphine from **1** followed by C−C bond activation of a second biphenylene molecule and rapid phosphine recoordination gives the Pt(IV) species **3**. Reductive C−C coupling

Scheme 2

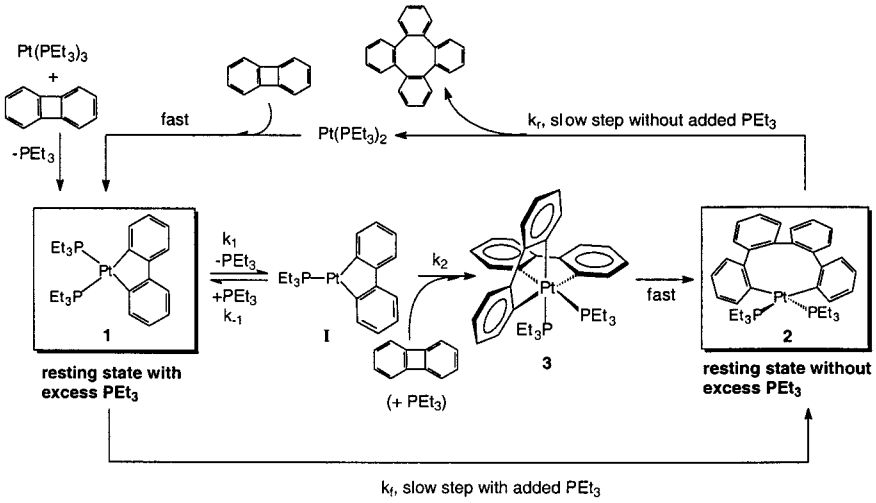

of adjacent aryl groups gives complex **2**.[11] Reductive elimination of tetraphenylene from **2** and subsequent rapid insertion of $(PEt_3)_2Pt$ into the C−C bond of biphenylene continues the cycle.

Clearly phosphine inhibits the catalytic formation of tetraphenylene. This inhibition is consistent with the reversible loss of phosphine from intermediate **1** to give a three-coordinate Pt(II) intermediate, **I**. **I** can then recoordinate to phosphine or cleave the C−C bond of biphenylene. The calculated branching ratio k_{-1}/k_2 of 131 indicates the preference of **I** for free phosphine vs biphenylene.

Kinetic analysis revealed that the ratio of free phosphine to biphenylene determined the overall rate and the resting state species of the catalytic cycle. Starting with **1**, a large excess of biphenylene, and no added phosphine, the resting state was complex **2**. That is, the rate of reductive elimination (k_r) of tetraphenylene from **2** determined the overall rate of catalysis. As free phosphine is added to the system, k_2 becomes the slow step in the cycle and complex **1** becomes the major resting state complex. Figure 3 reveals that as the PEt_3/biphenylene ratio increases the steady-state concentration of **1** increases relative to that of **2**.

The bulk of experimental and theoretical evidence suggests that phosphine loss occurs prior to reductive elimination in *cis*-bis(phosphine)$M^{II}R_2$ systems (M = Pd, Pt) where R is an alkyl group.[10,12,13] However, when at least one organic group is unsaturated, reductive elimination often occurs directly from the four-coordinate species without prior phosphine loss.[14] This appears to be the case in the present system, as addition of free phosphine had no effect on the rate of reductive elimination of tetraphenylene from complex **2**.[15] The ability to eliminate without phosphine dissociation has been explained, in part, by the decreased directionality of sp and sp^2 hybrid orbitals vs an sp^3 hybrid orbital. Decreased directionality of an orbital leads to increased multicenter bonding in the transition state and lower activation energies for reductive elimination.[16] For unsaturated organic fragments, experimental and theoretical evidence also indicates the involvement of a transient η^2 complex prior to loss of the organic species.[14] Consequently, unsaturated systems display enhanced thermal lability relative to that of the saturated systems. The structure of **2** shows a significant distortion toward a tetrahedral geometry, and it is possible that reductive elimination occurs by a continuation of this distortion without isomerization to a cis complex. Alternatively, the relatively high thermal stablity of complex **2** can be attributed to a large barrier for the rearrangement of the trans phenyl groups to a cis geometry, from which reductive elimination can occur.

C−C vs C−H Activation. There are only a few reported cases of intermolecular C−H bond activation of arenes by a phosphine-stabilized Pt(0) complex. In 1977, Stone et al. found that $Pt(P(cyclohexyl)_3)_2$ reacts with fluorobenzenes to give C−H oxidative addition products.[17] Whitesides and co-workers were able to activate the C−H bonds of a number of hydrocarbons (including benzene) using the reactive intermediate [bis(dicyclohexylphosphino)ethane]platinum(0).[18] The ability of aromatic hydrocarbons to coordinate in the η^2 mode prior to C−H activation has been demonstrated. For the case of [bis(dicyclohexylphosphino)ethane]platinum(0) there was evidence for an η^2-benzene complex prior to the C−H activation of benzene.[18a] Experimental evidence also suggests that C−H activation and η^2 coordination occur prior to the activation of

(11) A reviewer suggested that phosphine loss precedes reductive coupling in the Pt(IV) intermediate. The addition of 4 mM PEt_3, however, did not inhibit the rate of conversion of the Pt(IV) intermediate to **2**, which argues against prior phosphine dissociation. The low concentration of phosphine employed, however, does not completely discount this possibility. Kinetic studies using higher concentrations of PEt_3 could not be examined due to limitations in dynamic range in the NMR determinations.

(12) (a) Ozawa, F.; Ito, T.; Nakamura, Y.; Yamamoto, A. *Bull. Chem. Soc. Jpn.* **1981**, *54*, 1868−1880. (b) Gille, A.; Stille, J. K. *J. Am. Chem. Soc.* **1980**, *102*, 4933−4941. (c) Moravskiy, A.; Stille, J. K. *J. Am. Chem. Soc.* **1981**, *103*, 4182−4186. (d) Foley, P.; DiCosimo, R.; Whitesides, G. M. *J. Am. Chem. Soc.* **1980**, *102*, 6713−6725. (e) McCarthy, T. J.; Nuzzo, R. G. Whitesides, G. M. *J. Am. Chem. Soc.* **1981**, *103*, 3396−3403.

(13) Tatsumi, K.; Hoffmann, R.; Yamamoto, A.; Stille, J. K. *Bull. Chem. Soc. Jpn.* **1981**, *54*, 1857−1867.

(14) (a) Loar, M. K.; Stille, J. K. *J. Am. Chem. Soc.* **1981**, *103*, 4174−4181. (b) Brown, J. M.; Cooley, N. A. *Chem. Rev.* **1988**, *88*, 1031−1046 and references therin. (c) Ozawa, F.; Kurihara, K.; Fujimori, M.; Hidaka, T.; Toyoshima, T.; Yamamoto, A. *Organometallics* **1989**, *8*, 180−188. (d) Stang, P. J.; Kowalski, M. H. *J. Am. Chem. Soc.* **1989**, *111*, 3356−3362. (e) Calhorda, M. J.; Brown, J. M.; Cooley, N. A. *Organometallics* **1991**, *10*, 1431−1438. (f) Kohara, T.; Yamamoto, T.; Yamamoto, A. *J. Organomet. Chem.* **1980**, *192*, 265−274. (g) Abis, L.; Sen, A.; Halpern, J. *J. Am. Chem. Soc.* **1978**, *100*, 2915−2916.

(15) It is possible that phosphine dissociation from **2** is rate determining (i.e., recoordination of phosphine to form **2** is slow), and that trans-to-cis isomerization, phosphine recoordination, and reductive elimination are all rapid and irreversible. This would also lead to a lack of dependence of the rate of tetraphenylene formation on the phosphine concentration. We feel it is unlikely, however, that reaction of phosphine with the three-coordinate 14-electron intermediate would be slow.

(16) Low, J. J.; Goddard, W. A. *J. Am. Chem. Soc.* **1986**, *108*, 6115−6128.

(17) Fornies, J.; Green, M.; Spencer, J. L.; Stone, F. G. A. *J. Chem. Soc., Dalton Trans.* **1977**, 1006−1009.

(18) (a) Hackett, M.; Ibers, J. A.; Whitesides, G. M. *J. Am. Chem. Soc.* **1988**, *110*, 1436−1448. (b) Hackett, M.; Whitesides, G. M. *J. Am. Chem. Soc.* **1988**, *110*, 1449−1462.

Scheme 3

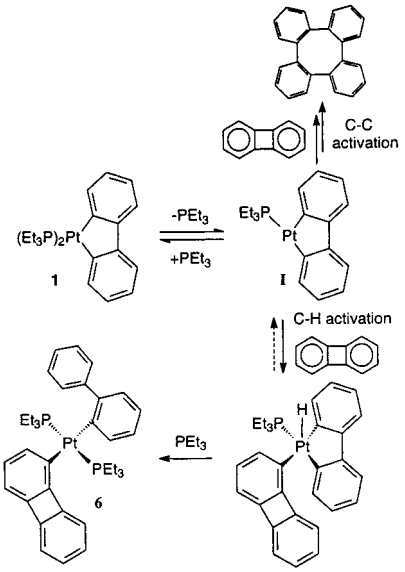

C−C bonds.[5b,19] In our case, there was no indication of η^2 coordination or C−H activation of benzene or biphenylene (prior to C−C cleavage) with the reactive species $[(PEt_3)_2Pt^0]$. However, it is very possible that η^2 coordination and C−H activation are *very fast and reversible* and therefore not observed on the NMR time scale. Halpern et al. demonstrated that *cis*-hydridoalkyl and -hydridoaryl bisphosphine complexes of platinum(II) undergo rapid reductive elimination of RH even at −25 °C.[14g] Furthermore, *trans*-$(PEt_3)_2PtH(C_6H_5)$ undergoes reductive elimination of benzene at 65 °C in C_6D_{12}.[20]

The formation of compounds **5** and **6** is consistent with C−H activation of benzene and biphenylene, respectively, by the Pt(II) complex **1**. Examples of nonelectrophilic C−H activation by a Pt(II) complex are rare, and often occur intramolecularly.[21] The formation of both of these complexes is inhibited by added phosphine, which is consistent with the loss of PEt_3 from **1** prior to C−H activation. A mechanism showing the formation of complex **6** is outlined in Scheme 3. The C−H activation of biphenylene is shown to occur at the α-carbon via intermediate **I**. This is consistent with the site of C−H activation of biphenylene by $(C_5Me_5)Rh(PMe_3)(Ph)(H)$.[19] The final step involves reductive elimination to give **6**.

If reversible C−H bond activation precedes C−C cleavage, the five-coordinate intermediate should exhibit a similar propensity to reductively eliminate the biphenyl group (giving **6**) as free biphenylene (dashed arrow, regenerating **I**). If this was the case, **6** would form at least as rapidly as tetraphenylene; however, this did not occur. One explanation may be that the C−C bond cleavage from **I**, which ultimately leads to the formation of tetraphenylene, does not require prior C−H activation of biphenylene. Rather, η^2 coordination may be kinetically and thermodynamically preferred over C−H activation. In this way, C−C activation is preceded by a series of η^2 coordination modes. The slow formation of **6** would be accounted for by the less frequent occurrence of C−H activation. The preference for η^2 coordination over C−H activation has been demonstrated in the reaction of the coordinatively unsaturated fragment $[(C_5Me_5)Rh(PMe_3)]$ with fused polycyclic arenes.[22] Complex **5** could form in a similar manner through reaction of **I** with benzene. The increased rate of formation of **5** relative to **6** is simply a result of the larger benzene concentration (vs biphenylene substrate).

Pd vs Pt Complexes. Both $Pd(PEt_3)_3$ and $(PEt_3)_2Pd$(2,2′-biphenyl) were capable of catalyzing the formation of tetraphenylene from biphenylene more efficiently than their Pt counterparts. In both cases, $(PEt_3)_2Pd$(2,2′-biphenyl) was the resting state species with no sign of $(PEt_3)_2Pd$(2,2′-tetraphenyl), the Pd analogue of complex **2**. Both of these observations are consistent with the catalytic cycle shown in Scheme 2. With the Pt system there was a near balance between k_f and k_r. Increasing the PEt_3:biphenylene ratio had the effect of decreasing k_f relative to k_r, resulting in complex **1** becoming the dominant resting state species. However, it is well-known that reductive elimination from Pd complexes is more facile than from Pt; therefore, reductive elimination from $(PEt_3)_2Pd$(2,2′-tetraphenyl) would be rapid. Consequently, the near balance that exists in the Pt system is eliminated (as k_r is now larger than k_f) and $(PEt_3)_2Pd$(2,2′-biphenyl) is the resting state species regardless of the phosphine concentration. The increased turnover rate results from k_f being more rapid in the Pd systems relative to the Pt systems. This arises from the weaker phosphine−Pd bond compared to the phosphine−Pt bond. Therefore, the three-coordinate Pd analogue of intermediate **I** is formed more rapidly than the Pt system, resulting in a larger k_f. Finally, no side products were observed when the reaction was run in C_6D_6. This is consistent with the decreased ability for Pd to C−H activate relative to Pt.

Conclusion

The electron rich species $Pt^0(PEt_3)_2$ and $Pd^0(PEt_3)_2$ are able to insert into the C−C bond of biphenylene. The resulting Pt(II) and Pd(II) complexes $(PEt_3)_2M$(2,2′-biphenyl) can also cleave the C−C bond of biphenylene with prior phosphine dissociation, resulting in a novel Pt(IV) species. The C−H bond of benzene and biphenylene can also be cleaved by $(PEt_3)_2Pt$(2,2′-biphenyl). In this study, carbon−carbon bond activation and formation were coupled in a catalytic reaction, resulting in the generation of tetraphenylene. The resting state species was found to vary with the *ratio* of biphenylene to free phosphine, rather than the absolute concentration of either. The results indicate that $(PEt_3)M$(2,2′-biphenyl) (M = Pt, Pd) has a much greater tendency to coordinate PEt_3 than cleave the C−C bond of biphenylene. The rate of catalytic formation of tetraphenylene is increased with Pd complexes relative to Pt complexes due to the more facile reductive elimination from Pd compounds. On the basis of the insights provided by this study, efforts are currently underway to maximize the catalytic turnover rate by varying the ligand system. The cleavage of C−C bonds in other substrates is also being examined.

Experimental Section

General Considerations. All manipulations were performed under an N_2 atmosphere, either on a high-vacuum line using modified Schlenk techniques or in a Vacuum Atmospheres Corp. glovebox. Tetrahy-

(19) Perthuisot, C.; Jones, W. D. *J. Am. Chem. Soc.* **1994**, *116*, 3647−3648.

(20) Arnold, D. P.; Bennett, M. A. *Inorg. Chem.* **1984**, *23*, 2110−2116.

(21) For intermolecular examples, see: Yamazaki, S. *Polyhedron* **1992**, *11*, 1983−1985. Uchimaru, Y.; El Sayed, A. M. M.; Tanaka, M. *Organometallics* **1993**, *12*, 2065−2069. For intramolecular examples, see ref g, 5h, and: Hietkamp, S.; Stufkens, D. J.; Vrieze, K. *J. Organomet. Chem.* **1979**, *168*, 351−361. Cavell, K. J.; Jin, H. *J. Chem. Soc., Dalton Trans.* **1995**, 4081−4089. Williams, N. A.; Uchimaru, Y.; Tanaka, M. *J. Chem. Soc., Chem. Commun.* **1995**, 1129−1130. Lopèz, O.; Crespo, M.; Font−Bardía, M.; Solans, X. *Organometallics* **1997**, *16*, 1233−1239.

(22) (a) Chin, M. R.; Dong, L.; Duckett, S. B.; Partridge, M. G.; Jones, W. D.; Perutz, R. N. *J. Am. Chem. Soc.* **1993**, *115*, 7685−7695. (b) Chin, M. R.; Dong, L.; Duckett, S. B.; Jones, W. D. *Organometallics* **1992**, *11*, 871−876. (c) Jones, W. D.; Dong, L. *J. Am. Chem. Soc.* **1989**, *111*, 8722−8723.

drofuran, benzene, and toluene were distilled from dark purple solutions of benzophenone ketyl. Alkane solvents were made olefin-free by stirring over H_2SO_4, washing with aqueous $KMnO_4$ and water, and distilling from dark purple solutions of tetraglyme/benzophenone ketyl. Benzene-d_6, toluene-d_8, and xylene-d_{10} were purchased from Cambridge Isotope Laboratories, and distilled under vacuum from dark purple solutions of benzophenone ketyl, and stored in ampules with Teflon-sealed vacuum line adaptors. The preparations of $Pt(PEt_3)_3$,[23] $Pd(PEt_3)_3$,[24] 2,2′-dilithiobiphenyl,[25] *cis*-$PtCl_2(PEt_3)_2$,[26] and $(depe)PtCl_2$[27] have been previously reported. Biphenylene was purchased from Aldrich Chemical Co., 2,2′-dibromobiphenyl was purchased from Alfa Aesar (Avocado), and triethylphosphine was purchased from Strem Chemical Co. The liquids were stirred over sieves, freeze−pump−thaw−degassed three times, and vacuum distilled prior to use.

All ^{1}H NMR and ^{31}P NMR spectra were recorded on a Bruker AMX400 spectrometer. All ^{1}H chemical shifts are reported in parts per million (δ) relative to tetramethylsilane and referenced using chemical shifts of residual solvent resonances (C_6D_6, δ 7.15; $CDCl_3$, δ 7.24; CD_2Cl_2, δ 5.32). ^{31}P NMR spectra were referenced to external 30% H_3PO_4 (δ 0.0). GC−MS was conducted on a 5890 Series II gas chromatograph fitted with an HP 5970 Series mass selective detector. Analyses were obtained from Desert Analytics. A Siemens SMART system with a CCD area detector was used for X-ray structure determination.

Preparation of $(PEt_3)_2Pt(2,2'$-biphenyl), 1. All glassware was thoroughly dried prior to use. A solution of 2,2′-dilithiobiphenyl (from 496 mg (1.59 mmol) of 2,2′-dibromobiphenyl) in ether (5 mL) was added dropwise to a stirred suspension of *cis*-$PtCl_2(PEt_3)_2$ (725 mg, 1.44 mmol) in 50 mL of benzene at room temperature. The mixture became green-yellow over the course of the addition. The reaction mixture was stirred for 3 h, during which time the color turned bright yellow. The reaction was quenched with 10 mL of H_2O. The organic layer was separated, dried with $MgSO_4$, and recrystallized (benzene/methanol) to give air stable yellow crystals (650 mg, 77% yield). The compound slowly decomposed in $CDCl_3$ over several days. ^{1}H NMR ($CDCl_3$): δ 7.501 (dd, J_{Pt-H} = 48.6, J_{H-H} = 7.2, J_{P-H} = 7.2 Hz, 2 H), 7.405 (d, J_{H-H} = 7.6 Hz, 2 H), 6.999 (t, J_{H-H} = 7.2 Hz, 2 H), 6.880 (t, J_{H-H} = 7.2 Hz, 2 H), 1.995(1:4:6:4:1 quintet, J_{H-H} = 7.5, J_{P-H} = 7.5 Hz, 12 H), 1.142 (1:2:2:2:1 quintet, J_{P-H} = 15.0, J_{H-H} = 7.5 Hz, 18 H). ^{31}P{^{1}H} NMR (C_6D_6): δ 8.44 (s, J_{Pt-P} = 1922 Hz). Anal. Calcd for $C_{24}H_{38}P_2Pt$: C, 49.39; H, 6.56. Found: C, 49.38; H, 6.38.

If water is present during the reaction to form $(PEt_3)_2Pt(2,2'$-biphenyl), white plates of $(PEt_3)_2Pt(2,2'$-biphenyl)HBr, **8**, are formed as a minor side product. The isolation and characterization of this compound by NMR spectroscopy, elemental analysis, and X-ray diffraction is given in the Supporting Information (see Figure 9).

Preparation of $(PEt_3)_2Pt(2,2'$-tetraphenyl), 2. $(PEt_3)_2Pt(2,2'$-biphenyl) (100 mg, 0.17 mmol) and biphenylene (36.5 mg, 0.24 mmol) were dissolved in dry benzene (∼5 mL) in an ampule under nitrogen, and the sample was heated to 80 °C for 4 h. The solvent was removed under vacuum and the solid dissolved in methylene chloride and layered with acetone. Clear air stable crystals were obtained at −20 °C (114 mg, 90% yield). ^{1}H NMR (CD_2Cl_2): δ 7.441 (d, J_{Pt-H} = 34.2, J_{H-H} = 7.2 Hz, 2 H), 7.372 (dd, J_{H-H} = 7.8, 1.8 Hz, 2 H), 7.077 (dd, J_{H-H} = 4.8 Hz, 1.2 Hz, 4H), 6.997 (t, J_{H-H} = 7.2 Hz, 2 H), 6.958−6.887 (m, 4 H), 6.826 (d, J_{H-H} = 7.6 Hz, 2 H), 1.087−0.915 (m, 12 H), 0.638 (1:4:6:4:1 quintet, J_{H-H} = 7.5, J_{P-H} = 7.5 Hz, 18 H). ^{31}P{^{1}H} NMR (C_6D_6): δ −0.44 (s, J_{Pt-P} = 3173 Hz). Anal. Calcd for $C_{36}H_{46}P_2Pt$: C, 58.77; H, 6.30. Found: C, 58.81; H, 6.20.

Preparation of $(PEt_3)_2Pt(2,2'$-biphenyl)Br_2, 4. $(PEt_3)_2Pt(2,2'$-biphenyl) (100 mg, 0.17 mmol) was dissolved in a minimum amount of benzene (∼5 mL). Degassed bromine (8.8 μL, 0.17 mmol) was added dropwise at room temperature to the stirred solution. A white precipitate formed immediately. The solution was stirred for 5 min, layered with diethyl ether, and put in a −20 °C freezer. The white crystals that formed were filtered and rinsed with diethyl ether (99.3 mg, 78% yield). ^{1}H NMR (C_6D_6): δ 8.837 (d, J_{H-H} = 8.0 Hz, 2 H), 7.337 (d, J_{H-H} = 6.0 Hz, 2 H), 7.039 (t, J_{H-H} = 7.6 Hz, 2 H), 6.947 (t, J_{H-H} = 6.4 Hz, 2 H), 1.808−1.638 (m, 12 H), 0.522 (1:4:6:4:1 quintet, J_{H-H} = 7.6, J_{P-H} = 7.6 Hz, 18 H). ^{31}P{^{1}H} NMR (C_6D_6): δ −11.44 (s, J_{Pt-P} = 1749 Hz). Anal. Calcd for $C_{24}H_{38}Br_2P_2Pt$: C, 38.78; H, 5.15. Found: C, 38.98; H, 5.03.

Preparation of Complex 3. A solution of 2,2′-dilithiobiphenyl (0.33 mmol) in ether (5 mL) was added dropwise to a stirred suspension of $(PEt_3)_2Pt(2,2'$-biphenyl)Br_2 (19.3 mg, 0.026 mmol) in 5 mL of benzene at room temperature. The reaction mixture was stirred for approximately 15 min. The suspension was quickly filtered through a frit to remove as much LiBr as possible. The solvent was removed under vacuum, and the resulting solid was left under high vacuum for 1.5 days. The solid was then dissolved in benzene, and a ^{31}P{^{1}H} NMR spectrum was acquired. Two distinct resonances were observed. The resonance at δ −0.44 (s, J_{Pt-P} = 3173 Hz) was assigned as complex **2**. The other resonance at δ −31.64 (J_{Pt-P} = 1242 Hz) was assigned as complex **3**. At room temperature, **3** disappeared with the concomitant formation of complex **2**.

Preparation of *trans*-$(PEt_3)_2Pt(\alpha$-biphenyl)(Ph)-d_6, 5-d_6. $(PEt_3)_2Pt(2,2'$-biphenyl) (75 mg, 0.146 mmol) was dissolved in dry C_6D_6 (∼1 mL) in a sealed NMR tube under nitrogen. The tube was heated to 130 °C for 7 days. The solvent was removed and the solid dissolved in a minimum of hot acetone. Clear, air stable crystals were obtained by slow cooling to room temperature and then to −20 °C (45 mg, 46% yield). ^{1}H NMR (THF-d_8): δ 7.712 (dd, J_{Pt-H} = 39.6, J_{H-H} = 6.8, 1.5 Hz, 1 H), 7.355−7.290 (m, 3 H), 7.237−7.174 (m, 1 H), 6.941−6.840 (m, 3 H), 1.431−1.305 (m, 6 H), 1.282−1.157 (m, 6 H), 0.845 (1:4:6:4:1 quintet, J_{H-H} = 7.6, J_{P-H} = 7.6 Hz, 18 H). ^{31}P{^{1}H} NMR (C_6D_6): δ 4.40 (s, J_{Pt-P} = 2871 Hz). Anal. Calcd for $C_{30}H_{38}D_6P_2Pt$: C, 53.97; H, 5.69. Found: C, 54.86; H, 6.62.

Isolation of *trans*-$(PEt_3)_2Pt(\alpha$-biphenyl)(α-biphenylenyl), 6. Several depleted catalytic reaction mixtures were combined, and the solvent was removed. The resulting solid was dissolved in CH_2Cl_2, and **6** was isolated by thick-layer silica chromatography with a 96:4 (v/v) solution of hexanes−acetone as eluent (R_f = 0.5). ^{1}H NMR (THF-d_8): δ 8.177 (d, J_{H-H} = 6.7 Hz, 1 H), 7.760 (d, J_{Pt-H} = 39.4, J_{H-H} = 7.4, 1 H) 7.420−7.160 (m, 5 H), 7.080−6.840 (m, 3 H), 6.700 (d, J_{H-H} = 6.3 Hz, 1 H), 6.630−6.500 (m, 2 H), 6.490−6.410 (m, 1 H), 6.390−6.290 (m, 1 H), 6.170 (d, J_{H-H} = 7.0 Hz, 1 H), 1.547−1.314 (overlapping multiplets, 12 H), 0.855 (1:4:6:4:1 quintet, J_{H-H} = 7.4, J_{P-H} = 7.4 Hz, 18 H). ^{31}P{^{1}H} NMR (C_6D_6): δ 5.02 (s, J_{Pt-P} = 2805 Hz). Anal. Calcd for $C_{36}H_{46}P_2Pt$: C, 58.77; H, 6.30. Found: C, 58.70; H, 6.21.

Preparation of (depe)Pt(2,2′-biphenyl), 7. All glassware was thoroughly dried prior to use. A solution of 2,2′-dilithiobiphenyl (from 156 mg (0.50 mmol) of 2,2′-dibromobiphenyl) in ether (5 mL) was added dropwise to a stirred suspension of $(depe)PtCl_2$ (215 mg, 0.455 mmol) in 30 mL of benzene at room temperature. The reaction mixture was stirred for 1 h, during which time the color turned bright yellow. The reaction was quenched with 10 mL of H_2O. The organic layer was separated and dried with $MgSO_4$ and the solvent removed under vacuum. The resulting solid was dissolved in CH_2Cl_2, and **7** was isolated by thick-layer silica chromatography with a 1:1 (v/v) solution of CH_2Cl_2/benzene as eluent as air stable yellow crystals (176 mg, 70% yield). ^{1}H NMR (THF-d_8): δ 7.562 (dd, J_{Pt-H} = 51.7, J_{H-H} = 7.6, J_{P-H} = 7.6 Hz, 2 H), 7.288 (d, J_{H-H} = 7.5 Hz, 2 H), 6.845 (t, J_{H-H} = 7.5 Hz, 2 H), 6.739 (t, J_{H-H} = 6.5 Hz, 2 H), 2.113−1.888 (m, 8 H), 1.806 (d, J_{H-H} = 12.2 Hz, 4 H), 1.142 (1:2:2:2:1 quintet, J_{P-H} = 16.2, J_{H-H} = 7.5 Hz, 12 H). ^{31}P{^{1}H} NMR (THF-d_8): δ 54.71 (s, J_{Pt-P} = 1830 Hz). Anal. Calcd for $C_{22}H_{28}P_2Pt$: C, 47.74; H, 5.83. Found: C, 47.68; H, 5.89.

Preparation of $(PEt_3)_2Pd(2,2'$-biphenyl). $(PEt_3)_3Pd$ (203 mg, 0.35 mmol) and biphenylene (80.1 mg, 0.53 mmol) were dissolved in dry benzene (∼5 mL) in an ampule under nitrogen. The ampule was heated to 68 °C for 14 days. The ^{31}P{^{1}H} spectrum showed only product and free PEt_3. The volatiles were removed under vacuum, and the solid

(23) Yoshida, T.; Matsuda, T.; Otsuka, S. *Inorg. Synth*. **1990**, *28*, 120−121.
(24) Kuran, W.; Musco, A. *Inorg. Chim. Acta* **1975**, *12*, 187−193.
(25) Gardner, S. A.; Gordon, H. B.; Rausch, M. D. *J. Organomet. Chem*. **1973**, *60*, 179.
(26) Parshall, G. W. *Inorg. Synth*. **1970**, *12*, 27−28.
(27) Booth, G.; Chatt, J. *J. C. S. A Inorg. Phys. Theor*. **1966**, *6*, 634−638.

Table 3. Summary of Crystallographic Data for 1, 2, 4, 5, 6, 7, and 8

crystal parameters	1	2	4	5	6	7	8
chemical formula	$C_{24}H_{38}P_2Pt$	$C_{36}H_{46}P_2Pt$	$C_{24}H_{38}Br_2P_2Pt$	$C_{30}H_{44}P_2Pt$	$C_{39}H_{49}P_2Pt$	$C_{22}H_{32}P_2Pt$	$C_{24}H_{39}BrP_2Pt$
formula weight	583.57	735.76	743.39	661.68	774.81	553.51	664.49
cryst syst	orthorhombic	triclinic	monoclinic	monoclinic	triclinic	monoclinic	orthorhombic
space group, Z	$Pna2_1$, 4	$P\bar{1}$, 2	$P2_1$, 2	$P2_1/n$, 8	$P\bar{1}$, 2	$C2/c$, 24	$Pnma$, 4
a, Å	14.08140(10)	10.404(2)	9.5953(4)	9.02730(10)	11.3813(3)	24.30280(10)	18.1731(2)
b, Å	16.4069(2)	10.453(2)	13.5058(6)	20.2102(4)	11.8826(3)	13.4616(2)	13.33980(10)
c, Å	10.34030(10)	16.837(2)	10.7168(5)	31.84380(10)	14.1814(4)	38.9163(2)	10.45720(10)
α, deg	90	81.965(9)	90	90	81.2980(10)	90	90
β, deg	90	83.164(9)	110.4420(10)	92.59	72.5350(10)	98.47	90
γ, deg	90	60.777(13)	90	90	78.4240(10)	90	90
vol, Å^3	2388.94(4)	1579.6(4)	1301.35(10)	5803.74(13)	1783.73(8)	12592.7(2)	2535.09(4)
temp, °C	−50	−80	−90	−90	−90	−80	−50
ρ_{calc}, g cm^{-3}	1.623	1.547	1.897	1.515	1.443	1.752	1.741
no. of data collected	14609	10121	5335	22380	10844	39390	15021
no. of unique data	5558	6606	1781	7480	7563	14858	3175
no. of params varied	250	353	154	607	379	676	154
$R_1(F_o)$, $wR_2(F_o^2)$ ($I > 2\sigma(I)$)	0.0217, 0.0439	0.0239, 0.0572	0.0284, 0.0702	0.0475, 0.0836	0.0543, 0.1278	0.0397, 0.0743	0.0224, 0.0480
$R_1(F_o)$, $wR_2(F_o^2)$ (all data)	0.0278, 0.0455	0.0265, 0.0582	0.0331, 0.0727	0.0707, 0.0902	0.0625, 0.1323	0.0436, 0.0753	0.0289, 0.0498
goodness of fit	0.950	1.023	1.079	1.082	1.038	1.367	1.071

was kept under vacuum to remove excess biphenylene. A brown-red solid was obtained (170 mg, 98% yield). A trace of tetraphenylene was also present and was not separated. ^{1}H NMR (C_6D_6): 7.671 (d, J_{H-H} = 7.3 Hz, 2 H), 7.537 (d, J_{H-H} = 7.2, J_{P-H} = 4.5, Hz, 2 H), 7.204 (t, J_{H-H} = 7.2 Hz, 2 H), 7.120 (t, J_{H-H} = 7.3 Hz, 2 H), 1.995-(1:4:6:4:1 quintet, J_{H-H} = 7.5, J_{P-H} = 7.5 Hz, 12 H), 1.142 (1:2:2:2:1 quintet, J_{P-H} = 15.1, J_{H-H} = 7.2 Hz, 18 H). ^{31}P{^{1}H} NMR (C_6D_6): δ 4.94 (s).

General Procedure for Catalysis. A solution containing the metal complex (0.027 M) and biphenylene (10 equiv, 0.27 M) was prepared in C_6D_6 and added to a resealable NMR tube. The NMR tube was heated at 120 °C in a constant-temperature oil bath thermostatically controlled (±0.5 °C). ^{1}H NMR spectra were obtained at various intervals to obtain the catalytic turnover number.

Kinetics of Reductive Elimination of Tetraphenylene from 2. Six sealed NMR tubes were prepared with varying concentrations of PEt_3 (0.49, 0.29, 0.15, 0.044, 0.022, and 0 M) in toluene-d_8. The concentration of **2** in each tube was maintained at 0.023 M. The NMR tubes were heated at 115.5 °C in a constant-temperature oil bath thermostatically controlled (±0.5 °C). Samples were removed from the baths at intervals and cooled to room temperature. ^{1}H NMR spectra were obtained, and thermolysis was followed for a minimum of 3 half-lives. The methyl peak of toluene-d_8 was used as an internal standard. The observed rate constant (k_{obs}) was independent of phosphine concentration. The average $k_{obs} = 2.34(11) \times 10^{-6}$ s^{-1}. The same reaction was performed three times at 130 °C in xylene-d_{10} with a phosphine concentration of 0.023 M. The average rate constant was $1.08(3) \times 10^{-5}$ s^{-1}.

Kinetics of Catalysis. Five sealed NMR tubes were prepared with varying concentrations of PEt_3 and biphenylene (see Table 2) in *p*-xylene-d_{10}. The concentration of **1** in each tube was 0.023 M. The NMR tubes were heated at 130 °C in a constant-temperature oil bath thermostatically controlled (±0.5 °C). Samples were removed from the baths at intervals and cooled to room temperature. ^{1}H NMR spectra were obtained, and thermolysis was followed until a steady-state concentration of **1** and **2** was attained. The methyl peak of *p*-xylene-d_{10} was used as an internal standard. The data for each experiment in Figure 3 were fit to eq 10 using a least-squares approach (using the solver tool in Microsoft Excel) in which k_{obs}, $[\mathbf{1}]_o$, and $[\mathbf{1}]_{ss}$ were allowed to vary. These values were then used to calculate $[\mathbf{2}]_{ss}/[\mathbf{1}]_{ss}$ (= $([\mathbf{1}]_o - [\mathbf{1}]_{ss})/[\mathbf{1}]_{ss}$), and k_r and k_f using eqs 11 and 12, respectively.

Derivation of Rate Expressions. In Scheme 1, the time-dependent concentration for **1** is governed by eq 5. Application of the steady-state approximation to [**I**] allows k_f to be written as in eq 6.

$$-\frac{d[\mathbf{1}]}{dt} = k_f[\mathbf{1}] - k_r[\mathbf{2}] \quad (5)$$

$$k_f = \frac{k_1}{1 + k_{-1}[PEt_3]/k_2[\mathbf{BP}]} \quad (6)$$

Once steady-state conditions are reached, the rate of disappearance of **1** is equal to its rate of formation (eq 7). From mass balance, the total quantity of **1** + **2** must remain constant, either at time t or once steady state has been achieved (eq 16). Solving eq 16 for [**2**] and eq 7 for $[\mathbf{2}]_{ss}$ and substitution into eq 5 gives eq 8, where $k_{obs} = k_f + k_r$. Integration of eq 8 gives eq 10, which describes the approach of [**1**] to steady state.

$$k_f[\mathbf{1}]_{ss} = k_r[\mathbf{2}]_{ss} \quad (7)$$

$$[\mathbf{1}]_t + [\mathbf{2}]_t = [\mathbf{1}]_{ss} + [\mathbf{2}]_{ss} \quad (16)$$

$$-\frac{d[\mathbf{1}]}{dt} = (k_{obs})([\mathbf{1}] - [\mathbf{1}]_{ss}) \quad (8)$$

$$[\mathbf{1}] = ([\mathbf{1}]_o - [\mathbf{1}]_{ss})e^{-k_{obs}t} + [\mathbf{1}]_{ss} \quad (10)$$

Equation 7 can be solved for k_f and substituted into the expression for k_{obs} (eq 17), which upon rearrangement gives eq 11. k_f is obtained by rearrangement of eq 7 to give eq 12.

$$k_{obs} = k_f + k_r = k_r([\mathbf{2}]_{ss}/[\mathbf{1}]_{ss}) + k_r \quad (17)$$

$$k_r = k_{obs}/(1 + [\mathbf{2}]_{ss}/[\mathbf{1}]_{ss}) \quad (11)$$

$$k_f = ([\mathbf{2}]_{ss}/[\mathbf{1}]_{ss})k_r \quad (12)$$

X-ray Structural Determination of 1, 2, 4, 5, 6, 7, and 8. Single crystals of **1** and **8** were mounted with epoxy on glass fibers, and immediately placed in a cold nitrogen stream at −50 °C on the X-ray diffractometer. Single crystals of **2**, **4**, **5**, **6**, and **7** were mounted under Paratone-8277 on glass fibers, and immediately placed in a cold nitrogen stream at −80 or −90 °C on the X-ray diffractometer. The X-ray intensity data were collected on a standard Siemens SMART CCD area detector system equipped with a normal focus molybdenum-target X-ray tube operated at 1.5 kW (50 kV, 30 mA) for **1** and **8** and 2.0 kW (50 kV, 40 mA) for the remaining crystals. A total of 1321 frames of data (1.3 hemispheres) were collected using a narrow frame method with scan widths of 0.3° in ω and exposure times of 10 s/frame using a detector-to-crystal distance of 5.09 cm (maximum 2θ angle of 56.54°) for all of the crystals except **5** and **7**, which were collected using exposure times of 30 s/frame. The total data collection time was approximately 6 h for 10 s/frame exposures, and 13 h for 30 s/frame exposures. Frames were integrated with the Siemens SAINT program to 0.75 Å for all of the data sets; however, weak data > 45° were omitted from the refinement of **4** and **5**. The unit cell parameters for all of the crystals were based upon the least-squares refinement of three-

dimensional centroids of >5000 reflections.[28] Data were corrected for absorption using the program SADABS.[29] Space group assignments were made on the basis of systematic absences and intensity statistics by using the XPREP program (Siemens, SHELXTL 5.04). The structures were solved by using direct methods and refined by full-matrix least squares on F^2. For all of the structures, the non-hydrogen atoms were refined with anisotropic thermal parameters and hydrogens were included in idealized positions, giving data:parameter ratios greater than 10:1. The Pt bound hydride in **8** was located from the difference Fourier map, and the positional and isotropic thermal parameters were refined. There was nothing unusual about the solution or refinement of any of the structures, with the exceptions of **5** and **7**. Both complexes crystallized in the monoclinic crystal system, and the space group assignments were $P2_1/n$ and $C2/c$ for **5** and **7**, respectively. For a Z value of 8, **5** crystallized with two independent molecules in the asymmetric unit. For a Z value of 24, **7** crystallized with three independent molecules in the asymmetric unit. Further experimental details of the X-ray diffraction studies are provided in Table 3. Positional parameters for all atoms, anisotropic thermal parameters, all bond lengths and angles, and fixed hydrogen positional parameters are given in the Supporting Information for all of the structures.

(28) It has been noted that the integration program SAINT produces cell constant errors that are unreasonably small, since systematic error is not included. More reasonable errors might be estimated at 10× the listed value.

(29) The SADABS program is based on the method of Blessing; see: Blessing, R. H. *Acta Crystallogr., Sect A* **1995**, *51*, 33−38.

Acknowledgment is made to the U.S. Department of Energy, Grant FG02-86ER13569 for their support of this work.

Supporting Information Available: Text describing the preparation of $(PEt_3)_2Pt(2,2'\text{-biphenyl})HBr$ and tables listing the crystallographic data, positional parameters, anisotropic thermal parameters, and bond lengths and angles (46 pages). See any current masthead page for ordering information and Web access information.

JA973368D